match no. 28 pp. 105-137 1992

THERMAL DISSOCIATIVE ADSORPTION INTERACTIONS FOR A SINGLE WATER MOLECULE ON Pt(211) SURFACE CLUSTER. EXTENDED HUCKEL CALCULATIONS.

G.L. Estiú, S. Maluendes, E.A. Castro and A.J. Arvia

Instituto de Investigaciones Fisicoquímicas Teóricas y Aplicadas (INIFTA), Facultad de Ciencias Exactas, Universidad Nacional de La Plata. Sucursal 4, Casilla de Correo 16, 1900 La Plata, Argentina.

(received: November 1991)

ABSTRACT

The enhacement of the thermal dissociative adsorption of a single H_2O molecule on Pt produced by a dislocation fault has been theoretically studied in relation to electrocatalytic reactions by means of the extended Hückel method. The Pt(211) surface was represented by a metal cluster approach.

The comparison of several reactivity descriptor parameters shows a decrease in activation energy for H_2O dissociation on stepped surfaces with respect to the flat ones. This fact and the influence of an external applied potential are explained on the basis of the molecular orbital interactions which are involved in chemisorption bonds of both reactants and products.

INTRODUCTION

Modelling surface structures always implies working with surfaces involving an ideal topology. In this case, the sites of each crystallographic feature become characterized by the number of nearest neighbour atoms[1,2]. Structurally distinguishable sites should have different adsorption binding energies (BE) for a particular adsorbate[3]. Many heterogeneous catalytic reactions rates have been also found to display strong structural selectivity[4].

At room temperature and atmospheric pressure the STM of real single crystal metal surfaces exhibit small flat domains together with terraces, steps, corners, kinks and vacancy sites. This situation becomes more complicated for polycrystalline materials, which involve the single crystal domains separated by boundaries and a high density of intrinsic and extrinsic defects. Then, it becomes a rather difficult task to attempt to describe, under these circumstances, the distribution energy of different adsorption sites on metal surfaces. Hence, due to the small dimensions of the homogeneous surface domains only an energetic effect delocalized over the entire surface becomes usually evident[1].

To advance in the knowledge of structural effects in heterogeneous catalysis, it seems to be of practical use to study, in a separated manner, the effect of the different topological features of a particular surface on the adsorption energy and adsorbate-substrate structures. Starting with an ideal single crystal structure the real metal surface can then be approached step by step by the inclusion of a new feature, which gradually increase the degree of complexity of the system. From the low index Miller planes, usually referred to as singular orientations, the simplest increase in complexity leads to vicinal orientations defined by a controlled number of surface defects.

Any metal surface of relevance for heterogeneous catalysis and electrocatalysis, should imply both structural and thermal stability up to the melting point when heating in either oxidizing or reducing ambients. Its stability should be retained even after the adsorption/desorption cycle of any catalytic poison[2]. In this respect, one of the simplest examples of an ideal metal surface which maintains its catalytic properties are those constituted of (211) vicinal orientations, which have been extensively studied in relation to their adsorptive properties by means of surface spectroscopies. This is the case, for instance, of site exchange of adsorbed oxygen on Pt(211) followed by TPD of isotopic oxygen[5], the orientation of adsorbed CO on Pt(211) studied through NEXAFS[6], and the chemical reactivity and oxidation rates of CO and H on Cu(211) investigated by means of AES[4]. These results obtained for adsorbates on well defined solid surface substrates encourage a theoretical study about the increase in surface reactivity produced by a dislocation fault as denoted by semiempirically calculated reactivity descriptor parameters. In this respect it is of interest to compare previous results, obtained for the adsorption of H_2O on Pt(100) and Pt(111) single crystal surfaces[7] to those obtained on Pt(211). The decrease in activation energy (AE) for the reaction H_2O ---- H_{ad} + OH_{ad} in the absence of charge transfer turns out to be more remarkable for negative applied potentials simulated through the proper shift of the valence orbital ionization potential[7]. This fact can be explained throughout the greater stabilization attained for the H adatom as a consequence of the unusually large number of d orbitals involved in the Pt-H adsorption bond[8].

It should be noticed that Pt(211) as any other ideal single crystal surface differs from real surface structures. Nevertheless,

idealized models involving surfaces with a defined number of steps or, in general, any kind of surface defects, are useful to attempt to diminish the gap between ideal flat low index crystallographic faces of single crystals and the complex surfaces that characterize the real metals.

THE CALCULATION METHOD

The following three aspects of the calculation procedure deserve particular comments, namely, the cluster approach for the metal surface, the reason for the use of the extended Hückel method, and the simulation of the applied electric potential.

1. The cluster approach

To calculate the energetic parameters related to the dissociative interaction of H_2O molecule on Pt(211) the clusters depicted in Figs. 1 and 2 were used to model the Pt(211) stepped surface, that is, Pt(s)-|3(111)x(100)| in Somorjai's notation[2]. It consists of a regular array of monoatomic steps with (100) orientation separated by three atom width terraces having a (111) structure[5,8,9], and is defined as a vicinal orientation[1]. Because of the local nature of surface interactions, the disturbance in electron distribution caused by the presence of adsorbates is efficiently screened[10,11]. Accordingly, the cluster approach for the metal surface results particularly useful for studying adsorption at low adsorbate coverages on ideal surfaces[7,10,12-16].

In order to approach the flat metal surface condition the cluster size has been chosen sufficiently large to approach the periodicity of the entire surface and to describe an equivalent enviroment for each possible adsorption site. Therefore, none of the Pt atoms directly

involved in adsorption bonds are influenced by cluster boundaries when a $(Pt)_{19}$ cluster for a Pt(111) surface, and a $(Pt)_{25}$ cluster for the Pt(100) surface are used (Fig. 3)[7]. However, it is not easy to avoid boundaries in a vicinal structure. According to the TLK model[1], vicinal surface structures can be analyzed in terms of only three main features, namely terraces consisting of strips of atomically smooth low-index planes; ledges made of one atom height steps, and kinks on the steps. When modelling these surfaces, the cluster approach requires a large number of atoms in order to represent the different adsorption sites free of boundary effect. Unfortunately, computational time sets the cluster size to 24 atoms (Fig. 1) where terraces become influenced by the cluster boundary. In order to overcome this drawback BE values calculated on flat surfaces modelled by means of the clusters depicted in Fig. 3 for terrace sites were compared to those resulting for atoms at the border and at the bottom of the step (atoms 1 and 2, Fig. 1).

2. The application of the extended Hückel method

The calculation is based on the EHM (EHM)[17,18], which has been used in previous theoretical catalytic studies[7,19,20]. The corresponding input parameters are given in Table 1. Diagonal elements of the hamiltonian matrix are expressed by the valence orbital ionization potentials of the atomic orbital (VOIP), while off diagonal elements are calculated by means of the weighted H_{ij} formula[21].

The EHM in its original form is useful for advancing in the understanding of chemical systems[22-24]. It has no limitations such as those of ab-initio quantum mechanical calculations for extended systems involving substrate-adsorbate interactions. Both the EHM and related methods such as ASED[25,26] provide reasonable qualitative trends in the dependence of the system properties as a function of either the applied

potential or the surface structure, although in other cases they fail, particularly when electrostatic interactions are excluded. This drawback, however, can be overcome by adding correction terms[27,28]. Hence, several approaches for the calculation of the interatomic repulsion energies are reported in the literature. Thus, according to Anders et al.[28] the repulsion energy, E_R, for each pair of atoms can be approximated by the equation:

$$E_R = A \exp(-rB) \qquad (1)$$

where A and B denote the repulsion parameters, and r is the corresponding internuclear separation. The value of E_R can be determined from the differences in the BE values when inner orbitals are either taken into account or neglected and has been considered to be pairwise additive[28-30].

For the electrochemical system the potential applied to the electrode can be simulated by shifting the valence band of the metal cluster which models the metal surface. This method of simulating the applied potential is justified in the following section.

A different BE value corresponds to each applied potential. Then, repulsion terms have to be obtained not only as a function of the interatomic separation but also of the metal cluster Fermi level shift.

For cluster modelled Pt surfaces, the coefficients A and B are obtained by substracting the values of BE calculated with the {5d6s} and the more extended (5p5d6s) basis set. As diagonal terms of the hamiltonian are modified when applied potentials are simulated, a different set of repulsion parameters is obtained for each potential[31]. Both dependences fit the equation:

$$E_R = C \exp(-rD)\exp(-KE) \qquad (2)$$

where r denotes the internuclear distance (in A) for a given pair of atoms, and E is the applied electrode potential (in V) calculated as the difference between H_{6s6s} and the standard 6s VOIP of Pt in vacuo, in agreement with the work function-applied potential one to one correlation.

Following this approach the corresponding repulsion energies, E_R(Pt-O) and E_R(Pt-H), were obtained by using the following approximate equations[31],

$$E_R(\text{Pt-O}) = 35867.970 \exp(-5.977\ r) \exp(-0.067\ E), \qquad (3)$$

$$E_R(\text{Pt-H}) = 174.354 \exp(-3.655\ r) \exp(-0.148\ E), \qquad (4)$$

It becomes evident that this approach makes unnecessary to include electrostatic repulsion correction terms when O-H bonding is considered because of the absence of extended internal orbitals in the atoms involved.

Due to the inclusion of repulsion terms, the Pt-H_2O and Pt-H distances and adsorption configurations have been semiempirically optimized throughout the geometry furnishing the minimum binding energy, resulting in a Pt-O distance of 2.0 Å for water adsorption. The Pt-Pt distance was set at 2.77 Å according to the geometry of the bulk metal[32,33]. For H_2O molecule, an OH bond length of 1.0 Å and a HOH angle of 104.5° were considered.

3. The simulation of the applied potential

Applied potentials are simulated with the valence band shift model[15] by either decreasing or increasing VOIP for positive or negative charging, respectively, as indicated elsewhere[7,19,20,34,35]. The resulting shift in d band level of Pt correlates to the actual electrode charging either negatively or positively. This approach, although a rather simplified one, has been used in semiempirical studies of electrochemical systems[7,19,20,34,35] or surface dopant effect[36,37], as it reflects the correct trend for the influence of the variation of the electrode potential on the properties of the system. The adsorption sites remain unchanged as the applied potential was modified within ±1.0 V range. As the present calculations are focussed to investigate trends of variation in the stabilization energies for different potentials applied to the metal, changes of ±1.0 V in VOIP have been arbitrarily correlated to changes of ±1.0 V from the zero potential, the latter being taken as the standard VOIP of the metal in vacuo.

The valence band shift model can be justified on the basis of the following experimental facts. The work function of the metal electrodes and other potential-dependent properties of the electrical double layer are conserved after emersion from the electrolyte solution[38-40], and the work function of the metal in the electrochemical environment and the applied potential fullfil a linear dependence[41] with a slope which is a characteristic of the system. This slope in some cases is equal to one[41,42]. In the present case, a one to one correlation was chosen because there is no other experimental evidence in favour of a different potential scale parametrization. The chosen correlation furnishes the correct trend in metal d band shifting with the applied potential.

MOLECULAR ORBITAL INTERACTIONS INVOLVED IN H_2O-Pt(211) ADSORPTION-DECOMPOSITION REACTION

1. The influence of the surface topography

As it has been previously made for Pt(100) and Pt(111) single crystal surfaces, H_2O molecule and H-atom adsorption sites have been selected as those which furnishes the minimum adsorption energy for the system.

The adsorption of H_2O molecule at a top site is favoured due to the directional characteristics of the corresponding $3a_1$ orbital which is involved in the adsorption bond through its delocalization on the d-band of Pt. However, new adsorption sites which imply linear coordination are defined when a dislocation fault appears, as now adsorption on the border of the step (atom 1) and adsorption on the trench (atom 2) should be considered. In addition, water can adsorb in a perpendicular configuration regarding either the (111) plane or the Pt (100) plane. Accordingly, four different configurations for adsorbed water (Fig. 4a) can be compared to linearly adsorbed water on Pt(100) and Pt(111) far from the step, in order to choose the adsorption sites most energetically favoured (Table 2). The water adsorption at the step border, where a quasi-Pt(100) site is involved, appears to be the most likely one in coincidence with the greater BE of H_2O on Pt(100) than on either Pt(111) or Pt(211) (Table 2). Nevertheless, it should be noted that the calculation procedure discriminate slightly between a tilted or a perpendicular configuration for the adsorbate when regarding the terrace (111) plane as reference. There are also several surface sites on the Pt(211) structure where the H atom can be adsorptively stabilized (Fig. 4b). Hollow (3-3) sites are energetically favoured for adsorption on terrace[7] (Table 2). Otherwise, for adsorption at the trench different distances either parallel to the

terrace between H atom and Pt (atom 1), or perpendicular to the second Pt(111) surface, define distinguishable sites for H atom adsorption (Fig. 4b).

When sites H_a, H_b, H_c and H_d are compared, the lowest adsorption energy comes out for the Pt (atom 1)-H atom distance equal to 1.6 Å parallel to the topmost surface (H_c). This geometry defines a tilted bridge adsorption bonding on the Pt(100) plane, and a distorted hollow (3-3) bonding on the Pt(111) plane (Fig. 4b). Both adsorption sites cooperate to the stabilization of the adsorbed H atom. This extre stabilization energy justifies the enhancement of the BE values for the H atom adsorption at the step (Table 2).

The H-atom adsorbs at the bottom of the step (trench) because of the extra orbital simultaneous interactions resulting between the H atom and the top and bottom Pt atoms of the step as depicted in Fig. 5. Accordingly, the specific geometry of the Pt(211) site allows the participation of d_{z^2}, d_{xy}, $d_{x^2-y^2}$ and d_{yz} orbitals in the adsorption interaction, in either an individual or a multicentric manner (Fig. 5). It should be also noticed that neither $d_{x^2-y^2}$ nor d_{xy} orbitals are involved in bond formation when H adsorbs on a different type of surface site[8]. This situation brings about a stability for adsorbed H atoms which becomes greater than that found in flat surfaces. Perhaps, H-atom adsorption site can be better described as a bicoordination structure emerging in the (100) strips, throughout Pt atoms 1 and 2 (Fig. 1). This is in agreement with the higher sticking probability for H-atoms on Pt(100) than on Pt(111), i.e. Pt(100) offers the most favourable adsorption site for H atoms.

The conclusion that H-atoms adsorbed at step sites involve a much more complex interaction than those occupying terrace sites has also been derived from PAX data (Photoelectron spectroscopy of adsorbed Xe),

which provide information about local variation of the electrostatic potential at the atomic scale[43]. In this case the "local work function" decreases 1.0 eV at the step sites resulting from a Pt(111) surface[44]. This decrease in the absolute value of the ionization potential results in a localized shift of the d-band of Pt upwards favouring the adsorption of H-adatom through an electron transfer from the metal to the adsorbate. As it is already known the lower the surface electrostatic potential the lower the activation barrier for charge transfer onto adsorbed species[44]. Accordingly, those situations involving adsorption at the step should imply an induced enhancement of the H_2O molecule dissociation by the metal surface structure itself.

After the H-Pt(211) and the H_2O-Pt(211) adsorption have been considered it is possible to choose a probable reaction pathway for the heterogeneous decomposition of H_2O without charge transfer which allows the comparison to the reaction undergoing on Pt(100) and Pt(111) in order to analyze the influence of the Pt topography on the adsorption energy of reactants and products (Table 2). In going from the initial to the final state the chemisorption energy of the system increases (Fig. 6) according to the gradual modification of water structural parameters. The resulting energy/distance profile is comparable to a reaction coordinate, and in this case the highest BE difference as referred to the initial adsorbed system can be regarded as the activation energy (AE) of the reaction.

The calculation method is not adequate to decide the reaction pathway involving the lowest energy values for the water decomposition reaction. However, a similar path can be postulated on each surface structure in order to analyze comparatively the energy involved in going from the initial to the final state on Pt(211), Pt(111) and

Pt(100), after selecting the adsorption sites of minimum energy for both the initial and final adsorbed systems. Thus, the reaction pathway refers to the simplest one that can be postulated in order to go from the initial to the final adsorbed configurations. The energy corresponding to the stabilization of products has a considerably influence on AE values.

Although calculations for H_2O molecule and H atom BE and water decomposition AE on flat Pt single crystal surfaces have been already made[7], they have been improved now by introducing changes in both the adsorption distances and the dissociation mechanism, which lead to a lowering of the activation energy. Both the primitive and the improved pathways proposed for H_2O decomposition on Pt(111) and on Pt(100) are comparatively depicted in Figs. 7a,b. Thus, in the primitive pathway, when the H_2O molecule OH bond lies parallel to the metal surface, its stretches out to dissociation, yielding a stable adsorbed H-atom when localized onto the energetically favoured adsorption site[7]. For the improved model the Pt-H adsorption distance which corresponds to the reactive OH bond parallel to the surface is 2.0 Å, i.e. the H-atom is too far from the metal surface to be stabilized by coordination. Torsional movement of water molecule, without angular deformation goes forward until the remaining OH bond locates perpendicular to the metal surface. Then, the stretching of the reactive OH bond furnishes the H-atom stabilization in the most favourable adsorption site, i.e. a hollow 3-3 site for Pt(111) or a bridge site for Pt(100). For this new configuration an increase in OH bond length occurs simultaneously with the shortening of the Pt-H bond distance. Then, according to the improved model, the AE decreases for Pt(111) and Pt(100) surfaces and the trend in AE variation remains as in the primitive approach, i.e. Pt(100)<Pt(111). It should be noted that in all cases the highest

energy intermediate is obtained before the equilibrium configuration for the Pt-H has been reached. Total energy of the adsorbed system decreases for increasingly important Pt-H interaction.

For a similar H_2O dissociation pathway on Pt(211), repulsive interactions between the H and the Pt atom located at the border of the step (atom 1 in Figs. 1 and 2) calculated according to equation (3) result in a greater stretching of the Pt-H bond during the O-H angular deformation to avoid an enhancement of the energy of the distorted H_2O molecule adsorbed on the Pt(211) surface which would yield a misleading AE value. In this case for the simple H_2O molecule deformation scheme described in the present work, the lowest energy reaction pathway corresponds to a constant Pt(atom 1)-H distance of about 1.6 Å. This figure becomes compatible with the minimum value of repulsive energy effects, and the most efficient Pt-H interaction at the reactive site (Fig. 6). For the uncharged Pt surface the maximum energy corresponds to the structure indicated by number 7, that is when the OH bond begins to stretch out. For further OH bond stretching the Pt-H interaction gradually increases so that the lowering of the energy of the adsorbed system is observed. Due to the convergence of several orbital interactions, and in agreement with the local surface potential decrease, the H-adatom stabilization energy becomes considerably greater for stepped Pt(211) surfaces lowering the value of AE and producing the enhancement of the H_2O molecule thermal dissociative reactivity (Table 2).

2. Changes in the thermal dissociative adsorption energy with the applied potential.

The AE barrier for H_2O molecule thermal decomposition on Pt(100) and Pt(111) changes when the VOIP values are shifted by applying an

external potential. Negative applied potentials produce specifically a reinforcement in the charge transfer mechanism of stabilization of water decomposition products i.e. adsorbed H and OH, which results in a decrease of the AE. This simple although approximate procedure for the applied potential simulation has been justified by several authors[7,15,19,20,34,35].

The influence of the applied potential either by shifting it positively or negatively, exhibits the same trend on the dissociative adsorption reactivity of Pt(211) as that already reported for Pt(100) and Pt(111) (Table 3), although the charge transfer to the H-adatom on the step becomes in this respect the most sensitive variable for the first surface structure owing to the confluence of non local and local ionization potential changes at this site.

Negative charging shifts the Fermi level upwards resulting in a non local effect that reinforces the local specific characteristics of the dislocation. The greater the H-atom stabilization, the lower the value of AE. Otherwise, the positive charging, as it displaces the Fermi level downwards, produces the opposite effect (Table 3, Fig. 8) Furthermore, it should be noticed that owing to the strong H-atom Pt-d orbital interaction on the stepped Pt(211) surface, displacements of metal-d band levels become sufficiently large to change the geometry of the intermediate from structure number 7 to structure number 8 (Fig. 6, Table 4). This change in the geometry is the consequence of the requirement of a longer O-H bond stretching to stabilize the H atom by locating it near the metal surface as the d band energy level decreases.

CONCLUSIONS

The reactivity of stepped Pt(211) surfaces for thermal dissociation of a single H_2O molecule into adsorbed OH and H was semiempirically analyzed in comparison to flat Pt(100) and Pt(111) surfaces. Calculated energies for the postulated intermediate state geometries demonstrate a lower energy of the activated complex on stepped than on flat surfaces.

The increase in the reactivity for the reaction on stepped Pt(211) can be justified through the greater stabilization of the H-atom resulting from the dissociation of a H_2O molecule due to its coordination on the most energetically favoured adsorption Pt site. Accordingly, the greatest capability of the step for the dissociation of the water molecule is compatible with extra orbital H-atom stabilizing interactions.

Results derived from the EHM calculations are in agreement with PAX measurements which show that the defect induced enhancement of the catalytic activity of metal surfaces, particularly for Pt(211), is due to a localized work function decrease in the step sites, which is absent on terrace sites, and results in a lowering of the activation barrier when charge transfer onto adsorbed species is involved.

The results of the present calculations also point out the possibility of adsorbate induced restructuring effects at the metal surface level. There are a few examples of electrochemical reactions at the submonolayer and monolayer levels which can produce severe modifications at single crystal noble metal electrodes (Pt and Au) in acid solutions caused by a single electroadsorption/electrodesorption cycle involving atoms (H, O, Cl)[45-50]. Comparable effects have also been observed for the same polycrystalline and preferred oriented metal electrode/electrolyte solution interfaces[51-54]. Therefore, although

the present calculations do not provide quantitative information involving surface restructuring, the adsorbate induced restructuring offers an interesting pathway which deserves further work to envisage a molecular level explanation of the precedent experimental facts. The adsorbate induced metal surface restructuring probably reflects the importance of lateral bonding forces at the adsorbate/substrate system.

ACKNOWLEDGEMENT

This research project was financially supported by the Consejo Nacional de Investigaciones Científicas y Técnicas and the Comisión de Investigaciones Científicas de la Provincia de Buenos Aires.

REFERENCES

1.- J. Bénard (editor), Adsorption on Metal Surfaces. An Integrated Approach, Studies in Surface Science and Catalysis, 13, Elsevier, Amsterdam, The Netherlands (1983).

2.- D.W. Blakely and G.A. Somorjai, Surface Sci., 65, 419 (1977).

3.- H.R. Siddiqui, X. Guo, I. Chorkendorft and J.T. Yates, Jr., Surface Sci., 191, L813 (1987).

4.- J.S. Arlow and D.P. Woodruff, Surface Sci., 180, 89 (1987).

5.- H.R. Siddiqui, A. Winkler, X. Guo, P. Haganns and J.T. Yates, Jr., Surface Sci., 193, L17 (1988).

6.- J. Somers, Th. Lindner, M. Surman, A.M. Bradshaw, G.P. Williams, C.F. McConville and D.P. Woodruff, Surface Sci., 183, 576 (1987).

7.- G.L. Estiú, S.A. Maluendes, E.A. Castro and A.J. Arvia, J.Phys. Chem., 92, 2512 (1988).

8.- H. Kobayashi, S. Yoshida, H. Kato, K. Fukui and K. Tarama, Surface Sci., 79, 189 (1979).

9.- H. Kobayashi, S. Yoshida, H. Kato, K. Fukui, K. Tarama and M. Yamaguchi, Surface Sci., 97, 329 (1980).

10.- Andzlem, Surface Sci., 108, 561 (1981).

11.- A. van der Avoird, H. de Graaf and R. Berns, Chem.Phys.Letters, 48, 407 (1977).

12.- A.B. Anderson, Surface Sci., 105, 159 (1981).

13.- J.E. Müller, Surface Sci., 178, 598 (1986).

14.- A. Gavezzotti, G.F. Tartadini and H. Miessner, J.Phys.Chem., 92, 872 (1988).

15.- S.P. Mehandru and A.B. Anderson, J.Phys.Chem., 93, 2044 (1989).

16.- V. Barone, Surface Sci., 189/190, 106 (1987).

17.- R. Hoffmann, J.Chem.Phys., 39, 1397 (1963).

18.- J. Howell, A. Rossi, D. Wallace, K. Haraki and R. Hoffmann, Forticon 8, program N°344, QCPE, Cornell University, Ithaca, New York.

19.- G.L. Estiú, S.A. Maluendes, E.A. Castro and A.J. Arvia, J. Electroanal.Chem. (submitted).

20.- G.L. Estiú, S.A. Maluendes, E.A. Castro and A.J. Arvia, J. Electroanal.Chem. (submitted).

21.- J.M. Ammeter, H.B. Bürgi, J.C. Thibeault and R. Hoffmann, J.Am. Chem.Soc., 100, 3686 (1978).

22.- G. Calzaferri, L. Forss and I. Kamber, J.Phys.Chem., 93, 5366 (1989).

23.- R. Hoffmann, Angew.Chem., 94, 725 (1982).

24.- W. Tremel and R. Hoffmann, Inorg.Chem., 26, 118 (1987).

25.- A.B. Anderson, J.Chem.Phys., 62, 1187 (1975).

26.- A.B. Anderson, R.W. Grimes and S.Y. Hong, J.Phys.Chem., 91, 4242 (1987).

27.- A.B. Anderson and R. Hoffmann, J.Chem.Phys., 60, 4271 (1974).

28.- L.W. Anders, R.S. Hansen and L.S. Bartell, J.Chem.Phys., 59(10), 5277 (1978).

29.- A. Gavezzotti and M. Simonetta., Surface Sci., 99, 453 (1980).

30.- E. Ortoleva and M. Simonetta, J.Mol.Struct. (Theochem.), 149, 161 (1987).

31.- G.L. Estiú and S.A. Maluendes, Z. für Chemie (submitted).

32.- C. Minot, B. Bigot y A. Hariti, J.Am.Chem.Soc., 108, 196 (1986).

33.- Handbook of Chemistry and Physics, 55th edition, CRC Press Cleveland, Ohio (1973).

34.- A.B. Anderson and N.K. Ray, J.Phys.Chem., 86, 488 (1982).

35.- A.B. Anderson and D.P. Onwood, Surface Sci., 154, L261 (1895).

36.- A.B. Anderson and M.K. Awad, J.Am.Chem.Soc., 107, 7854 (1985).

37.- N.K. Ray and A.B. Anderson, Surface Sci., 125, 803 (1983).

38.- D.M. Kolb and W.N. Hansen, Surface Sci., 79, 205 (1979).

39.- W.N. Hansen, Surface Sci., 101, 109 (1980).

40.- W.N. Hansen, D.M. Kolb, D.L. Rath and R. Wille, J.Electroanal. Chem., 110, 369 (1980).

41.- D.M. Kolb, D.L. Rath, R. Wille and W.N. Hansen, Ber.Bunsen.Ges. Phys.Chem., 87, 1108 (1983).

42.- E.R. Kötz, H. Neff and K. Müller, J.Electroanal.Chem., 215, 331 (1986).

43.- K. Wandelt, J.Vac.Sci.Technol., A2(2), 802 (1984).

44.- S. Daiser y K. Wandelt, Surface Sci., 128, L213 (1983).

45.- P.N. Ross and F.T. Wagner, in Advances in Electrochemistry and Electrochemical Engineering, H. Gerischer and C.W. Tobias, eds., Vol. 13, p. 69, Wiley, New York (1984).

46.- Y. Nakai, M.S. Zei, D.M. Kolb and G. Lehmpful, Ber.Bunsenges. Phys.Chem., 88, 340 (1984).

F.T. Wagner and P.N. Ross, J.Electroanal.Chem., 150, 141 (1983).

47.- D. Aberdam, R. Durand, R. Faure and F. El-Omar, Surf.Sci., 171, 303 (1986).

48.- S. Hagstrom, H.B. Lyon and G.A. Somorjai, Phys.Rev.Letters, 15, 491 (1965).

49.- A.T. D'Agostino and P.N. Ross, Surf.Sci., 185, 88 (1987).

50.- J. Wiechers, T. Twomey, D. Kolb and R.J. Bohm, J.Electroanal. Chem., 248, 451 (1988).

51.- S.A. Bilmes, M.G. Giordano and A.J. Arvia, Canadian J.Chem., 66, 2259 (1988).

52.- M.E. Folquer, N.R. de Tacconi, J.R. Vilche and A.J. Arvia, J.Electrochem.Soc., 126, 257 (1979).

53.- S.A. Bilmes, M.C. Giordano and A.J. Arvia, J.Electroanal.Chem., 225, 183 (1987).

54.- C. Alonso, R.C. Salvarezza, J.M. Vara and A.J. Arvia, Electrochim.Acta, submitted.

TABLE 1.- Parameter used in the EHM calculation

Orbital	H_{ii} (eV)	μ_1	μ_2	c_1	c_2
5d Pt	-12.590	6.013	2.616	0.6334	0.5512
6s Pt	-10.000	2.554			
6p Pt	- 5.475	2.554			
1s H	-13.600	1.300			
2s O	-32.300	2.275			
2s O	-14.800	2.275			

H_{ii} = valence orbital ionization potential at the AO_i

μ_1, μ_2 = exponents in the STO.

c_1, c_2 = coefficients in the double zeta d orbitals of Pt.

TABLE 2.- Adsorption binding energies (BE) for a single H_2O molecule and a single H atom on Pt(111)[7], Pt(100)[7] and Pt(211). For the latter structure adsorbed configurations depicted in Fig. 4 have been considered. Activation energies (AE) for H_2O dissociation into H and OH adsorbates has been calculated for the most stable adsorption geometry on each surface structure.

Surface Structure	Adsorption geometry	Water BE (eV)	H-atom BE (eV)	AE (eV)
Pt(111)	on top	0.630	——	1.837
	hollow 3-3	——	3.717	——
Pt(100)	on top	0.740	——	1.501
	bridge	——	4.043	——
Pt(211)	wa Fig.4a	0.701	——	1.283
	wb Fig.4a	0.606	——	——
	wc Fig.4a	-0.325	——	——
	wd Fig.4a	-0.331	——	——
	Ha Fig.4b	——	7.182	——
	Hb Fig.4b	——	7.487	——
	Hc Fig.4b	——	7.315	——
	Hd Fig.4b	——	7.397	——

TABLE 3.- Calculated activation energies for the H_2O molecule dissociation into H and OH adsorbates on Pt(211) for different applied potentials. The latter are given in terms of H_{ii} for the Pt 6s orbital.

H_{ii}(6sPt)/eV	EA/eV
-9.00	0.9909
-10.00	1.2825
-11.00	1.6023
-12.00	1.9858

TABLE 4.- Energy values for each stage involved in the dissociation of the H_2O molecule into H and OH adsorbate on stepped Pt(221), according to the reaction pathway depicted in Fig. 6. The applied potential is expressed through the values of H_{ii} for the Pt 6s orbital.

Stage	H_{ii}/eV -9.00	-10.00	-11.00	-12.00
1	-2967.087	-3215.053	-3464.025	-3714.094
2	-2967.077	-3215.041	-3464.018	-3714.083
3	-2966,840	-3214.753	-3463.680	-3713.677
4	-2966.572	-3214.437	-3463.314	-3713.259
5	-2966.270	-3214.051	-3462.821	-3712.662
6	-2966.057	-3213.822	-3462.583	-3712.425
7	-2965.849	-3213.539	-3462.254	-3712.082
8	-2966.299	-3213.695	-3462.207	-3711.906
9	-2967.839	-3214.824	-3462.965	-3712.344
10	-2968.621	-3215.458	-3463.455	-3712.666
11	-2968.922	-3215.759	-3463.715	-3712.864

LEGENDS FOR THE FIGURES

Figure 1.- Cluster used to model Pt(211) surface structures. • topmost layer atoms, ◦ second layer atoms, o third layer atoms.

Figure 2.- Pt(211) structure. Squared atoms correspond to the surface atoms represented in Fig. 1.

Figure 3.- Metal clusters used to model different Pt surface sites. Full lines represent the topmost surface layer and dotted lines the second metal layer. a) clusters used to model a top site, a bridge site and (3-1) hollow site of Pt(111) surface; b) cluster used to model a (3-3) hollow sites of Pt(111); c) cluster used to model a top site, a bridge site and a hollow site of a Pt(100) surface.

Figure 4.- Lateral view of the Pt(211) surface structure. a) H_2O adsorption configurations which are compared for selecting that of minimum adsorption energy. b) H atom adsorption sites which are considered to find out that of minimum adsorption energy.

Figure 5.- a) Pt(211) orbitals which contribute to H-Pt bond; b) multicentric interactions.

Figure 6.- Steps involved in H_2O decomposition reaction on a stepped surface. Geometries are the same for charged and uncharged surfaces. In this case energy values correspond to the uncharged cluster surface.

Figure 7.- Energies involved in the different steps proposed for adsorbed H_2O decomposition. a) Pt(111); b) Pt(100).

——— first proposed mechanism[7]

------ second proposed mechanism

Figure 8.- Energy variation calculated as the difference between the energy of each H_2O molecule decomposition step and the energy of the adsorbed system. The activation energy increases with positive charging as the activated complex modifies its geometry. The reaction coordinate is defined as the distance between the reactive H-atom and the center of mass of the remaining ensamble.

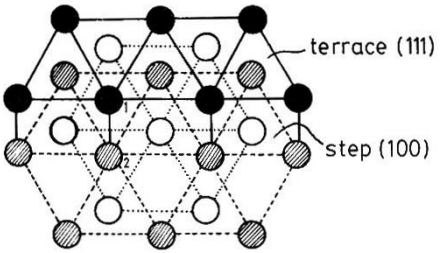

Fig. 1

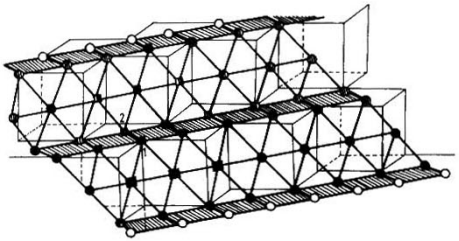

Fig. 2

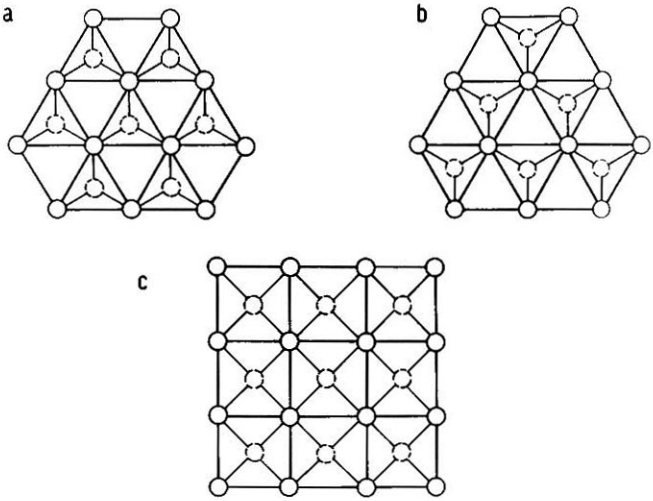

Fig. 3

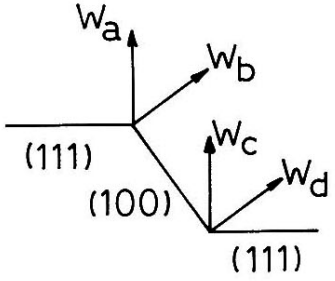

(a)

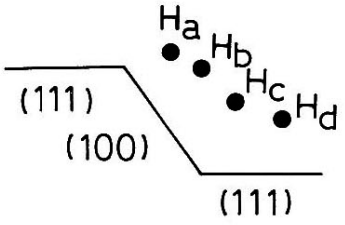

(b)

Fig. 4

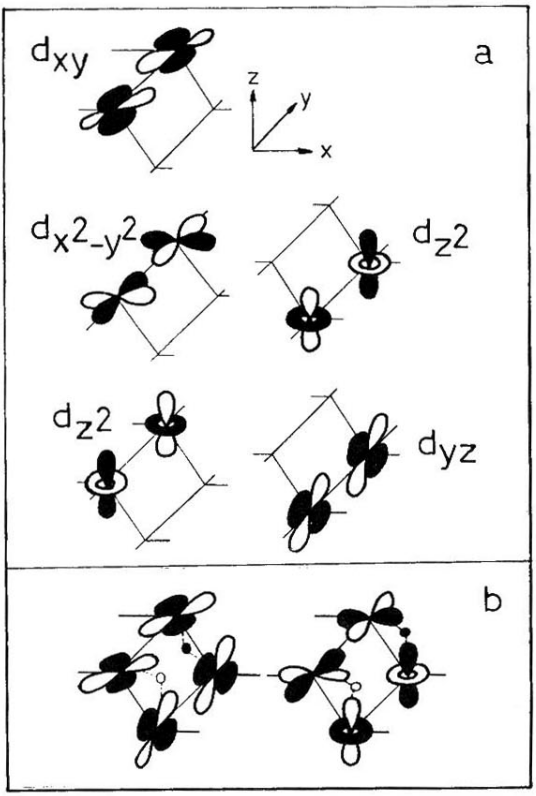

Fig. 5

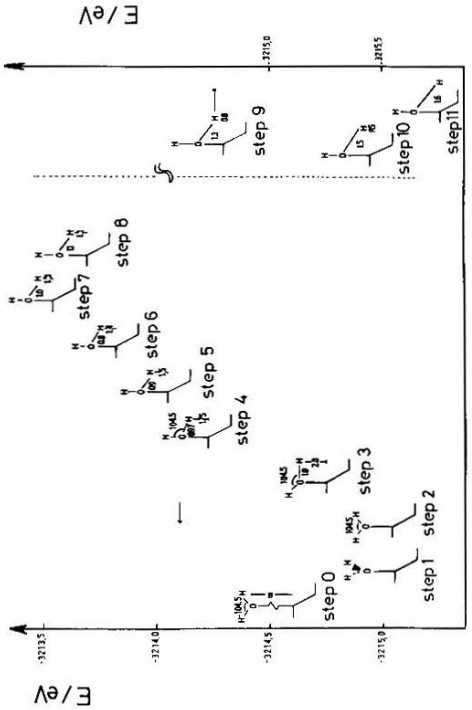
E / eV
-32135
-32140
-32145
-32150
-32155
step 0
step 1
step 2
step 3
step 4
step 5
step 6
step 7
step 8
step 9
step 10
step11
E / eV

Fig. 6

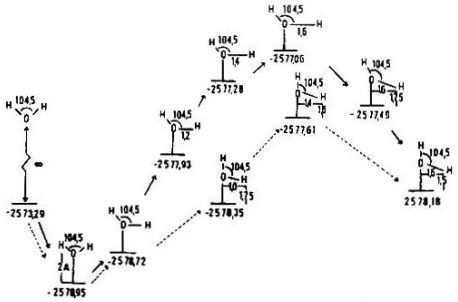

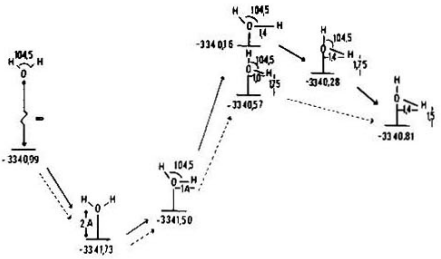

Fig. 7

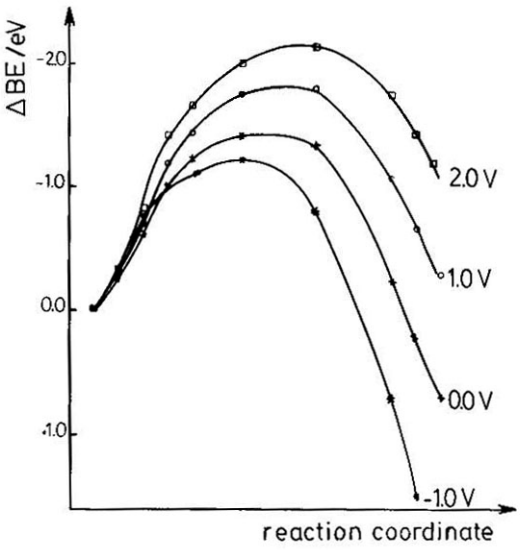

Fig. 8